

TAPERED DOUBLE CANTILEVER BEAM FRACTURE
TESTS OF PHENOLIC-WOOD ADHESIVE JOINTS¹
PART I. DEVELOPMENT OF SPECIMEN GEOMETRY; EFFECTS OF
BONDLINE THICKNESS, WOOD ANISOTROPY AND
CURE TIME ON FRACTURE ENERGY

Robert Ebewele

Research Assistant
Materials Science Program
Engineering Research Building
University of Wisconsin, Madison, WI 53706

Bryan River

Forest Products Technologist
Improved Adhesives Systems
U.S. Forest Products Laboratory
P.O. Box 5130, Madison, WI 53705

James Koutsky

Professor, Chemical Engineering
Department of Chemical Engineering
University of Wisconsin, Madison, WI 53706

(Received 9 March 1979)

ABSTRACT

Tapered double cantilever beam specimens were developed and used to test the effects of bondline thickness, wood anisotropy, and cure time on the fracture energy of phenolic-wood adhesive joints. Fracture energy, G_{Ic} , increases slowly with bondline thickness (in the range 160–100 microns) then jumps considerably (100–90 microns), and finally drops sharply at bondline thicknesses less than 70 microns. As the grain orientation with respect to the bonded surface (grain angle) is increased from zero degrees, G_{Ic} decreases and goes through a minimum at about 20 degrees grain angle. At larger grain angles, G_{Ic} increases. The fracture energy also increases strongly with cure time, reaching a plateau at long cure times.

Keywords: Tapered double cantilever beam, fracture energy, bondline thickness, grain angle, cure time, phenol-resorcinol.

INTRODUCTION

For many years it has been recognized that in order to design adhesive-bonded structures, there was a critical need to develop reliability criteria for adhesive joints. Essentially there are three basic modes of transferring loads between members of an adhesive-bonded assembly: Mode I—opening or cleavage mode, Mode

¹ We wish to thank the Nigerian Government, Weyerhaeuser Corporation, and the Forest Products Laboratory (Department of Agriculture) in Madison for providing generous support for this research. We especially wish to thank Dr. Roland Kreibich of Weyerhaeuser for his helpful advice and critical comments during the course of this investigation.

We also wish to thank Dr. Robert Gillespie, Dr. George Myers, and Dr. Alfred Christiansen of the Adhesives Section of the Forest Products Laboratory in Madison for their guidance and suggestions.

II—in plane shear, and Mode III—tearing or transverse shearing mode. In the wood industry, efforts for establishing these criteria (adhesive joint strength and durability) have tended to be based largely on results from shear and tension tests. This is obvious, from the fact that ASTM standards for testing of adhesive joints in bonded wood structures have been established for shear (D-905, C-906) and tension (D-897, C-297), while no such standards are available for cleavage tests. However, testing wood structures in shear or tension is beset with a number of problems as has been pointed out by various authors (Strickler and Pellerin 1973; Johnson 1973):

1. Stress concentrations are inherent in the test specimens because of the geometry of specimens and the methods of loading employed.
2. The ability of a specimen to reproducibly reflect the actual condition of the bond over the section under test may depend more upon the stress distribution peculiar to the specimen than upon the variables under investigation.
3. Failure may be initiated in conventional test specimens by stresses other than those nominally considered under evaluation.
4. Rigid adhesive bonds are strongest in shear, somewhat weaker in tension, and weakest in cleavage and peel. As a result, wood failure is obtained in shear and tension tests in properly formed joints. While high wood failure is an indication of strong adhesive bonds, use of percent wood failure as a sole criterion of bond quality is open to question, since cleavage stresses in such samples are usually not well controlled. Furthermore, while the amount of wood failure is useful in ranking strength of different adhesives, it tells us nothing about the strength of the adhesive itself under the most stringent conditions of cleavage loading.
5. Many samples are needed in lap shear testing to obtain reliable, statistically significant data. This is due to the lack of control of flaw sizes, grain angle orientations, etc., which are inherent in wood and complicate the fracture process.

Rigid adhesive joints are particularly susceptible to brittle failures. The rationale for a cleavage test, therefore, is the desire to simulate the peripheral stresses encountered on glued wood specimens during weathering. These stresses exert a prying or wedging effect.

The fracture mechanics approach to evaluate adhesive strength and durability has been found to be a useful tool, especially when dealing with rigid, brittle resin systems [Bascom et al. 1975; Mostovoy and Ripling 1975; Gledhill and Kinloch 1974]. The philosophy of this approach is to destructively test the adhesive bond system that has been purposely preflawed with a large, sharp, reproducible crack. The test is done under carefully controlled conditions to minimize scatter in the values of loading needed to propagate the crack. It has been found in such testing programs that brittle resins are particularly susceptible to cleavage failures.

Although previous workers in wood research have used fracture methods to evaluate the quality of bond, relatively few have attempted to use the double cantilever beam experiment that has been found quite successful in determining durability of metal bonding. Previous workers in fracture mechanics of wood have been concerned with the load to propagate a crack and the crack growth rate under a constant or variable load using a uniform double cantilever beam as

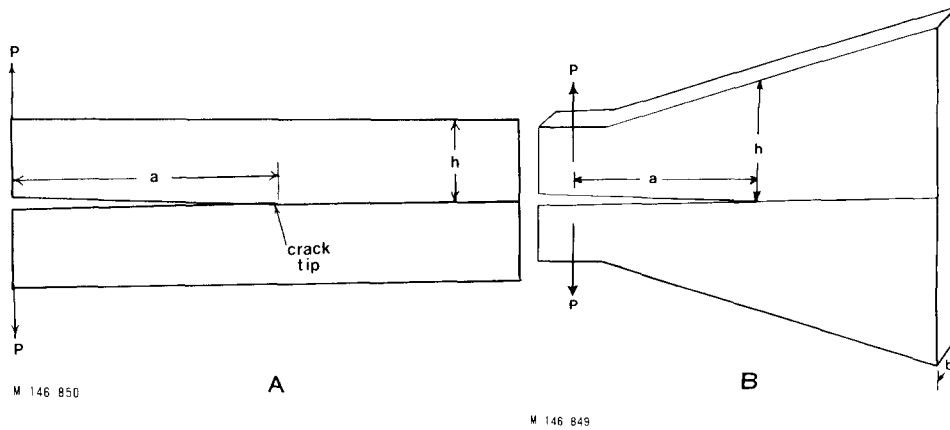


FIG. 1. Double cantilever beam specimens; (a) uniform beam ($h = \text{constant}$), (b) contoured beam ($h = \text{variable}$, dependent upon value of m).

shown in Fig. 1A. This type of work has been recently summarized by Ruedy [1977].

Following Griffith's (1920) work on brittle fracture and the subsequent modifications proposed by Irwin (1958), Ripling, Mostovoy and Patrick (1964) have designed contoured (tapered) double cantilever beam specimens for cleavage tests. The critical strain energy release rate under mode I is given by the following relation:

$$G_{Ic} = \frac{P_c^2}{2b} \left(\frac{\partial C}{\partial a} \right) \quad (1)$$

where:

G_{Ic} = critical strain energy release rate under mode I or cleavage load

P_c = critical load necessary to initiate crack extension

a = crack length

b = width of beam

C = compliance of specimen.

From the formulas of strength of materials for two cantilever beams with uniform height h , bending modulus E , and span equal to the crack length a , $\partial C/\partial a$ is given by:

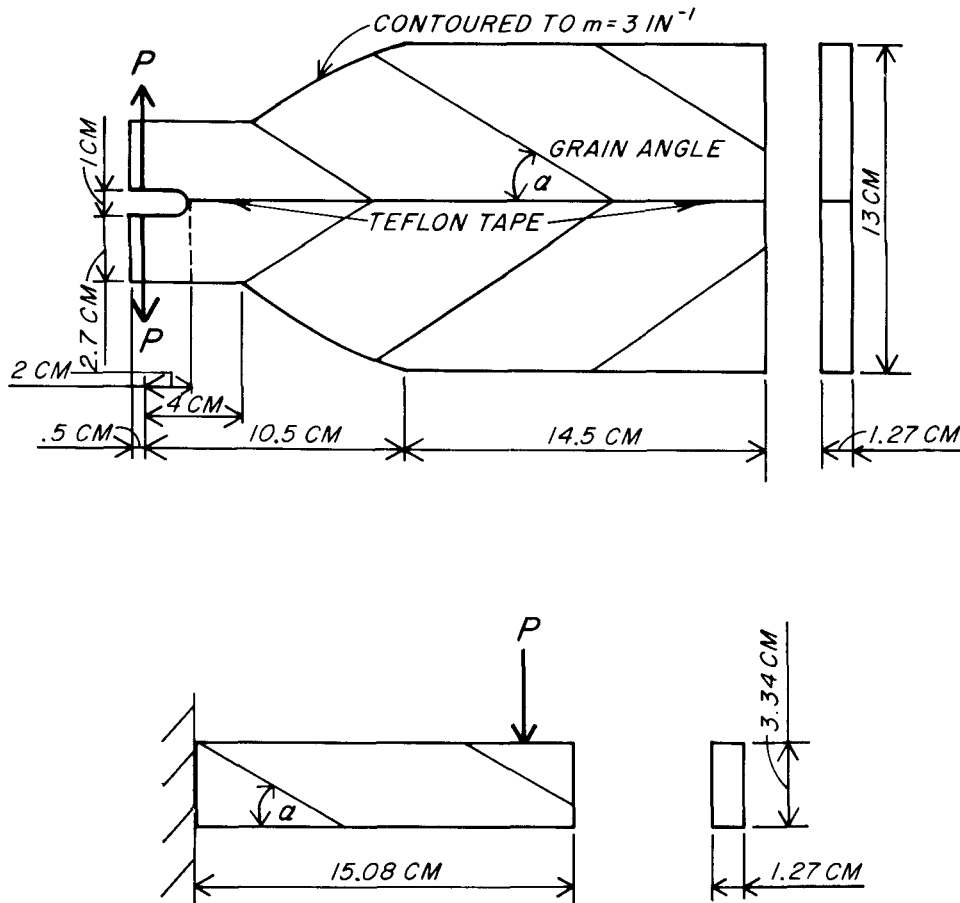
$$\frac{\partial C}{\partial a} = \frac{8}{Eb} \left[\frac{3a^2}{h^3} + \frac{1}{h} \right] \quad (2)$$

Thus:

$$G_{Ic} = \frac{4P_c^2}{Eb^2} \left[\frac{3a^2}{h^3} + \frac{1}{h} \right] \quad (3)$$

or

$$G_{Ic} = \frac{4P_c^2}{Eb^2} [m] \quad (4)$$



M 146 851

FIG. 2. Sample geometry used in these experiments. Note: Wood grains are oriented at an angle to the plane of the bondline with the exception of zero grain angle specimens. Contoured section of specimen corresponds to 40–110 mm from the point of applied load, P .

Equation 3 requires simultaneous measurement of both P_c and a for each calculation of G_{Ic} . However, if beams are contoured so that compliance changes linearly with crack length (i.e. $[m]$ is a constant), testing can be much simplified. This is achieved by varying the specimen height such that the quantity in the bracket in Eq. 4 is a constant (Fig. 1B), i.e.

$$[m] = \frac{3a^2}{h^3} + \frac{1}{h} = \text{constant}. \quad (5)$$

Equation 1 is derived assuming certain limitations on the sample. For instance, the thickness, b , of the sample must be large enough to assure plane strain conditions throughout the cross-section of the sample (Irwin 1958; Williams 1969; Cottrell 1959). Normally this can be achieved for brittle resins when b is 0.02 cm

or greater. If b is made too small, then plane stress effects can become important, and the crack does not propagate in a simple cleavage stress field. The resulting load measurement, P_c , does not give G_{Ic} directly but some combination of G_{Ic} and shear fracture energies. The deformation of the resin prior to fracture is assumed to be small, i.e., a brittle resin, in order for this analysis to be correct (Cottrell 1959; Bennett et al. 1965). Another practical assumption is that the crack propagates through the specimen as shown in the bondlines in Fig. 1.

The beam bending modulus is usually assumed to be isotropic, which is the usual case for most beam materials. This does not imply that orthotropic materials such as wood cannot be studied. For these cases the grain orientation of both beams should be the same for this simple analysis. Therefore, for the case of bonding two anisotropic adherends such as two pieces of wood, the same basic principles are involved. The crack will normally follow the bondline unless the wood beams are weak enough to cause the crack to propagate into the wood beams themselves. Of course, that condition of wood failure indicates either a good adhesive bond, having superior strength than wood itself or a weak wood structure in the beam.

When the uncracked portion of the beam becomes equal to or less than 1.5 times the height of the beam at that point, the back end of the beam begins to control the compliance. In this case the simple mechanics equations used in deriving Eq. 1 do not hold. One simple expedient is to lengthen the specimen as shown in Fig. 2 and to verify the predicted compliance expressions to ensure that the strength of materials solutions are valid for the specimen geometry chosen. The shape of the beam in the tapered section is chosen to make the beam strong enough so it will not break during testing. For metal beams, $[m]$ is chosen to be 11.81–35.43 cm^{-1} (30 to 90 inch^{-1}), while for polymers $[m]$ values of 0.39 to 3.94 cm^{-1} (1–10 inch^{-1}) have been used [Bascom 1975; Mostovoy and Ripling 1975; Ripling et al. 1964].

This work involves the bonding of tapered wood beams by a phenol-resorcinol adhesive and the subsequent fracture of such specimens. The objectives were to evaluate the technique to see if it could be reasonably applied to typical wood gluing procedures, and find the effects of bondline thickness, wood grain orientation, and cure time on fracture energy.

EXPERIMENTAL

Adherends

Hard maple, (*Acer saccharum*, Marsh) was chosen as the wood substrate to examine first, since it was of high modulus, and glue assimilation by the wood is minimal and can be controlled. Rough lumber for the specimens was conditioned to equilibrium at 23 C–44% RH ($\approx 8\%$ EMC). After reaching equilibrium, the lumber was jointed on one side and planed to the chosen thickness of 1.27 cm (0.5 inch). Samples were then cut to the shape shown in Fig. 2 (top). For most specimens we chose m values of 1.18 cm^{-1} (3 inch^{-1}). Some specimens were contoured to 0.52 cm^{-1} (1.33 inch^{-1}). These m values assured strong beams, resistant to breakage. Most samples were cut so the grain angle, α , to the bondline was maintained at 20 degrees as indicated in Fig. 2 (top). This was to assure that the fracture would remain in the bondline. For the study of grain variation, some samples were cut with α varying from 0 to 90 degrees. (Values of α greater than

90 degrees were avoided to ensure that the crack would not easily propagate into the wood beams.

The surfaces of the beams to be glued were carefully jointed by a sharpened 3 blade knife jointer. The wood beams were placed in a constant temperature, 23 C-44% humidity room for 3-4 days for conditioning.

The bending modulus of the wood was measured by the simple cantilever beam deflection method, Fig. 2 (bottom). The wood beams were cut from the contoured specimens that were used in the cleavage experiments. These specimens were cut with grain angles, α , varying from 0 to 90 degrees.

Adhesive

A phenol-resorcinol resin, Koppers G4411-A, was mixed with wood flour hardener G4400-B in the weight ratio of 100 grams resin and 20 grams hardener. The adhesive was mixed vigorously by hand for 10 min. The pot life of the resin was 3-4 h at room temperature.

Bonding

The adhesive was hand-brushed on both surfaces of the two beams to be mated assuring as uniform spread as possible. Open assembly times were kept very short, less than 15 sec. The beams were assembled and a small "Mylar" or "Teflon" film of thickness $2.54 \cdot 10^{-3}$ cm (1 mil) was inserted near the jaws of the specimens (see Fig. 2) to provide a large pre-crack flaw.

The assembled samples were placed in a press that could hold three double beam samples. (See Fig. 3A.) The closed assembly time was approximately 30 min. Samples were positioned so that the noncontoured sections could be put under pressure via the clamping press. Pressure was measured using a ring deflection load cell. Glueline pressures were held at 1.03-1.172 MPa (150-170 psi) during bonding. Note that the pressure is not uniform since it was applied only to the noncontoured sections. This gave samples of varying bondline thickness, which was found to be useful in evaluating the effects of bondline thickness on fracture energy. A modified press that gave a more uniform pressure and therefore more uniform bondline thicknesses was also employed and is shown in Fig. 3B. A third press configuration for holding two $m = 0.52 \text{ cm}^{-1}$ samples is shown in Fig. 3C. This last configuration gave extremely good control of bondline thickness over the entire bond length. Excess glue that exuded from the joint was scraped off with a knife before the adhesive was cured.

The press with samples was placed into a forced air oven at $70 \text{ C} \pm 1 \text{ C}$ for cure time of 25 min. to 20 h. The suggested cure time for this resin by the manufacturer was 25 to 30 min. The bulk of the data reported here was for those suggested cure times. However, in subsequent studies, cure time was found to be a significant factor and therefore longer cure times were also investigated. All samples were removed from the oven and from the press and conditioned at 23 C, 44% humidity for 3-4 days before fracture testing.

Fracture testing

A Riehle (Ametek) universal testing machine was employed for the cleavage fracture tests. Precision on the load measurements was ± 0.01 kg. The load was applied by knife edge grips as shown in Fig. 4, and the sample deflection at the

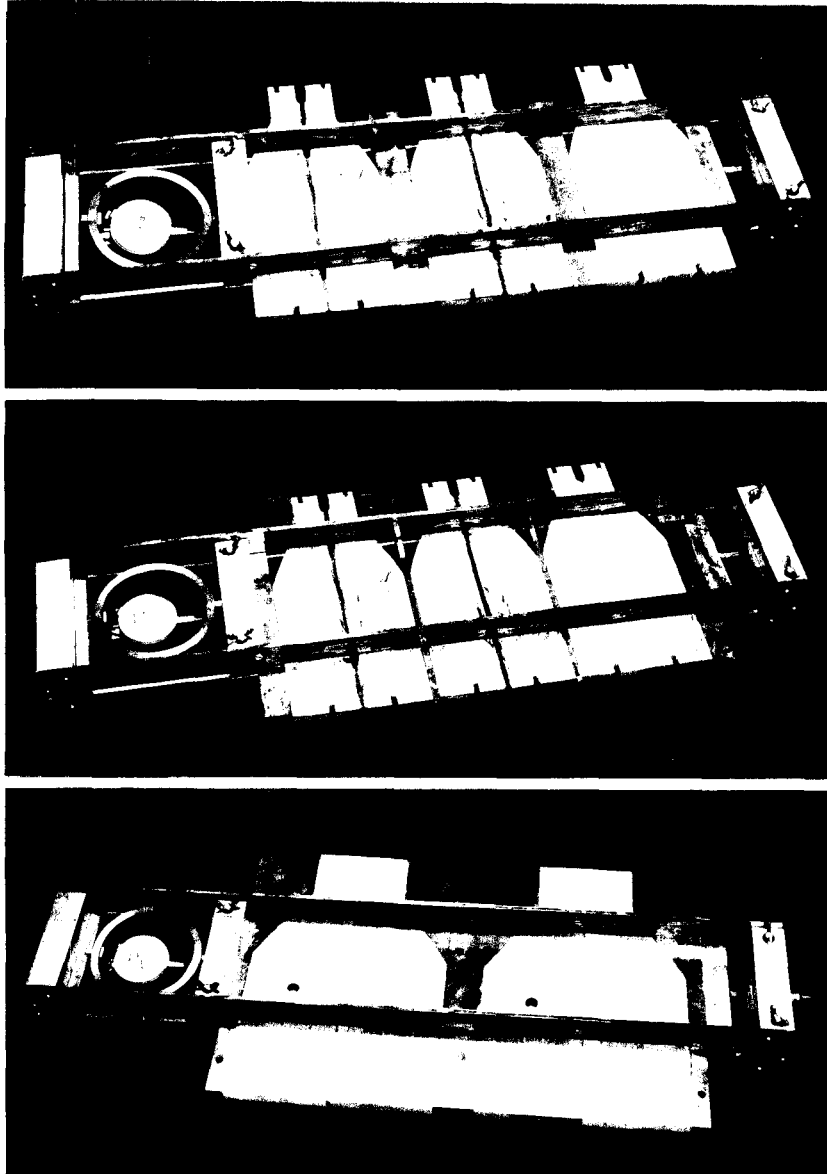


FIG. 3. Press designs for specimen preparation. Presses were capable of holding three specimens at the same time. Press A: bondline thickness in contoured section varied along specimen. Press B: variation of bondline thickness in contoured section of beam was minimized. Press C: Design for two cantilever beam specimens where $m = 0.52 \text{ cm}^{-1}$ for the contoured region.

applied load point was measured by an LVDT transducer mounted directly on one of the beams of the sample. The load and strain measurements were recorded on an x-y plotter from which P_c and P_a values could be readily obtained. Various crosshead speeds were used, but 0.2 mm/min. was found to be most satisfactory.

Bondline thickness measurements were made by a dual, linear traveling, recording microscope capable of ± 3 micron resolution. More than six measure-



FIG. 4. Specimen mounted with knife-edged grips in preparation for cleavage test. Position of knife edge of grips corresponds to $a = 0$.

ments of bondline thickness at 20-mm intervals were made for each sample on both sides of the sample to obtain the bondline thickness profile before fracture testing.

Crack lengths were also measured by hand, using both a rear-lighted sample and a light-colored sawdust powder pressed lightly to the side surface of the joint. As the crack would jump, the powder would fall off the sample indicating the location of the crack to within ± 3 mm, and detection of the rear light was usually observed about 1–3 mm behind the leading crack edge. Although these methods are crude when compared to other methods, they were of sufficient precision to be useful for the experiments involving variable bondline thickness.

RESULTS AND DISCUSSION

Typical bondline thickness measurements for samples pressed only on the non-tapered section are shown in Fig. 5A. These variable bondline thickness samples gave loads to fracture that increased on the crack propagated through the contoured region even though $\delta C/\delta a$ was constant. Figure 6A shows the raw load-deflection data for a typical, variable bondline-thickness sample. The fracture initiation energy, G_{Ic} , can be estimated from the load maxima, P_c , from Eq. 4. The corresponding bondline thickness was estimated by interpolation from the crack length and the measured bondline thickness shown in Fig. 5A.

Usually the initial pre-crack load propagation values were larger than the succeeding values. This was due to the fact that the "Mylar" or "Teflon" film

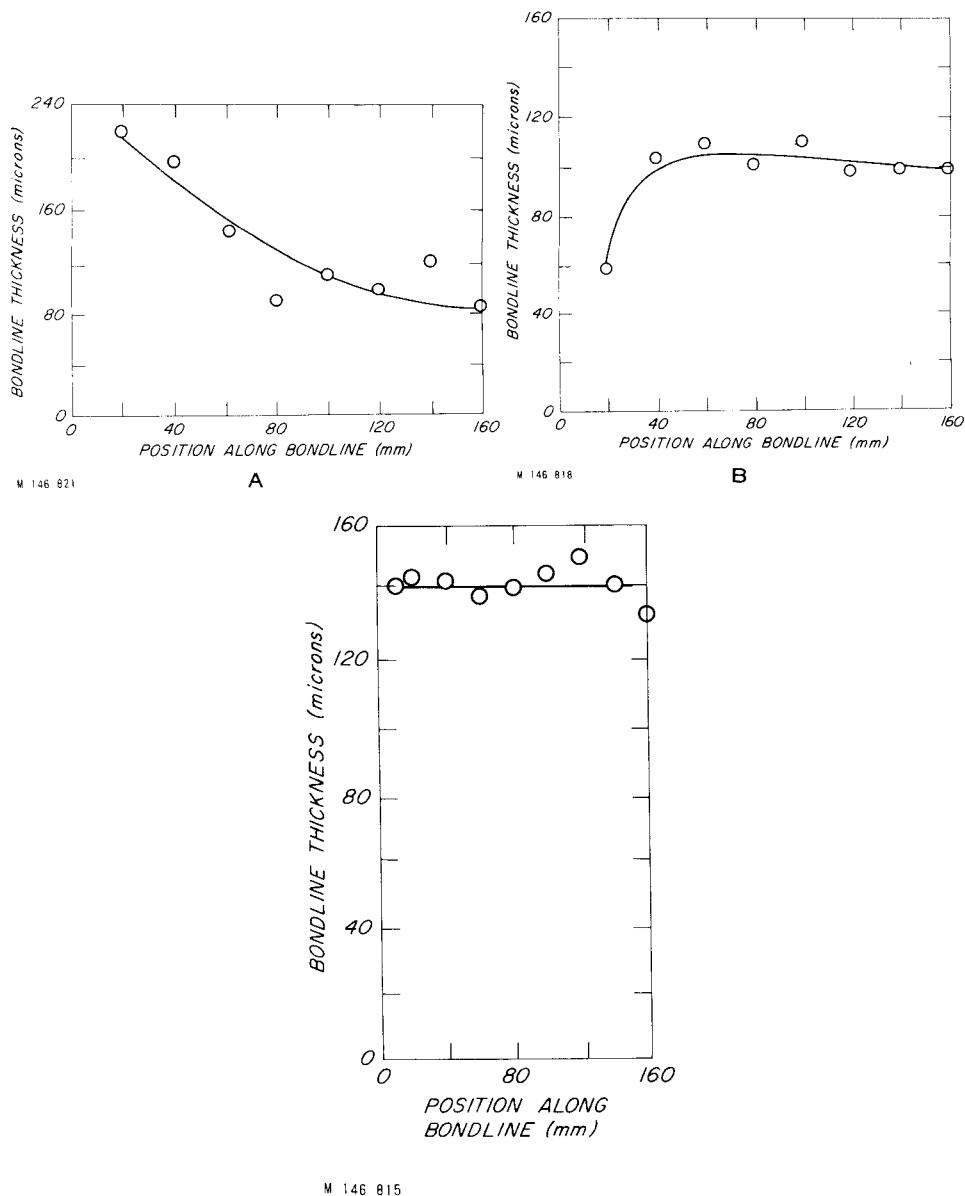


FIG. 5. (A) For the press design shown in Figure 3A, the bondline thickness decreases with increasing distance along the bondline. This was due to the variability of glueline pressure along the specimen. (B) For the press design shown in Figure 3B, the bondline thickness remains fairly constant in the contoured section. A more uniform glueline pressure is achieved by using the press design in Figure 3B. These results were typical for these specimens. (C) For the press design shown in Fig. 3C, the bondline thickness of the specimens remains constant throughout the contoured section.

produced only a blunt crack. As the crack initially propagated under load, it became much sharper, and hence the loads to propagate the sharp crack should be lower because of higher stress concentrations. One to three crack jumps appeared necessary to produce a sharp crack into the contoured region. If the

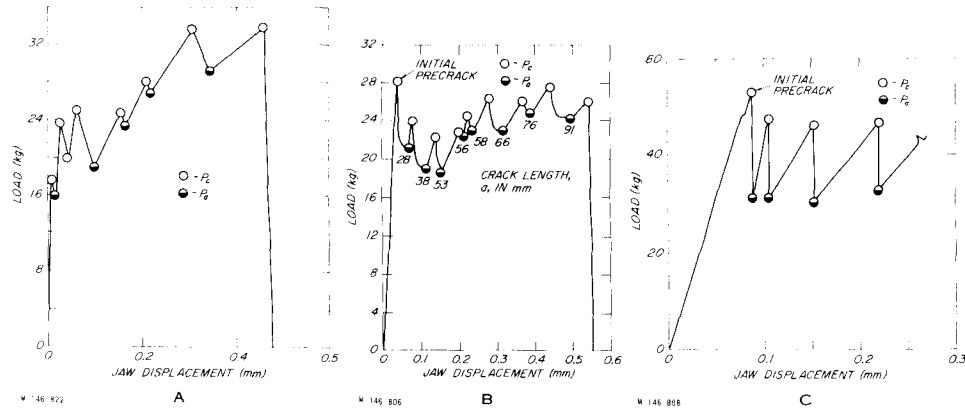


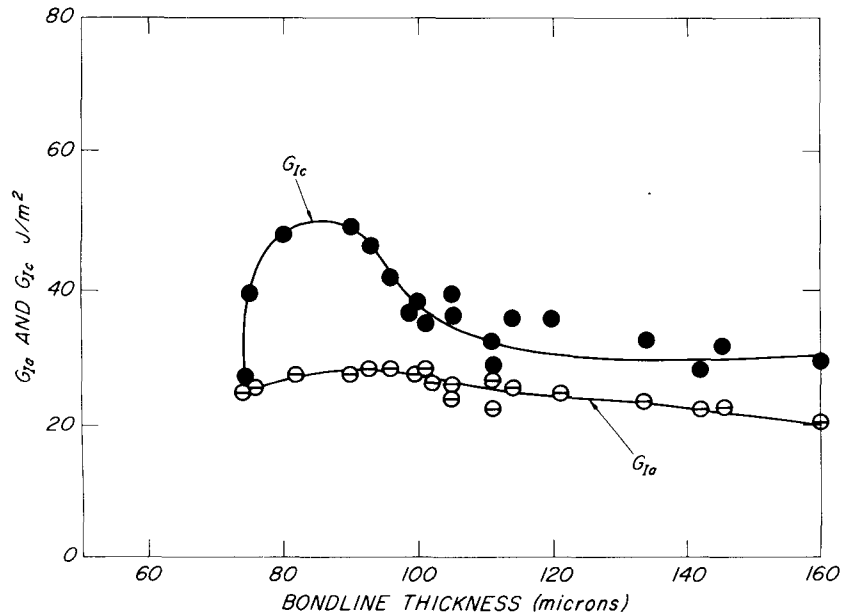
FIG. 6. (A) Load deflection data for a typical cleavage test on a specimen made in the press design shown in Fig. 3A where $m = 1.18 \text{ cm}^{-1}$ (3 inch^{-1}), $\alpha = 20^\circ$. Note increase of P_c and P_a . (B) Load deflection data for a typical cleavage test on a specimen made in the press design shown in Fig. 3B where $m = 1.18 \text{ cm}^{-1}$ (3 inch^{-1}), $\alpha = 20^\circ$. Note that the variability of P_c and P_a is not as severe as Fig. 6A. (C) Load deflection data for a typical cleavage test on a specimen made in the press design shown in Fig. 3C where $m = 0.52 \text{ cm}^{-1}$ (1.33 inch^{-1}), $\alpha = 20^\circ$. Note that P_c and P_a show even less variability than Fig. 6B.

bondline thickness was constant and a sharp crack was propagating, then the peak load values should remain the same. This was observed as seen in Figs. 6B and particularly Fig. 6C where the crack was in the contoured section and the fracture initiation loads, P_c , became constant. Once the crack approached the end of the contoured section, catastrophic failure of the whole sample was observed.

The saw-toothed character of the load-deflection data of Fig. 6 is indicative of unstable crack growth, i.e. whenever the load (or energy stored in the beam) reached a critical value P_c (or G_{1c}), the crack propagated at a faster rate than the crosshead speed until enough energy was lost to bring the crack to rest. The arrest load value (or energy) is designated by P_a (or G_{1a}). Thus for unstable crack growth $P_c > P_a$ (i.e. $G_{1c} > G_{1a}$). If $P_c = P_a$ (i.e. $G_{1c} = G_{1a}$), then a stable crack growth would be observed and the load-deflection data would essentially be a continuous, horizontal line.

Effect of bondline thickness

Samples were prepared with variable bondline thicknesses. Typical G_{1c} and G_{1a} values obtained from three samples are plotted in Fig. 7. Each point represents a fracture energy obtained from a measured P_c value. If the cure of the resin and bondline thickness are carefully controlled, the reproducibility on fracture energy measurements can be within $\pm 10\%$ for samples prepared by the press design shown in Fig. 3A. As the bondline thickness is reduced from 160 to 100 microns, G_{1c} slowly increases. At 90–100 microns, a considerable jump in fracture energy is observed. If bondline thickness is reduced beyond 70–80 microns, a decrease in fracture energy is observed. This interesting result corresponds with data from lap shear or block shear tests where optimum bondline thicknesses for greatest strength have also been observed for conventional thermosetting wood adhesives.

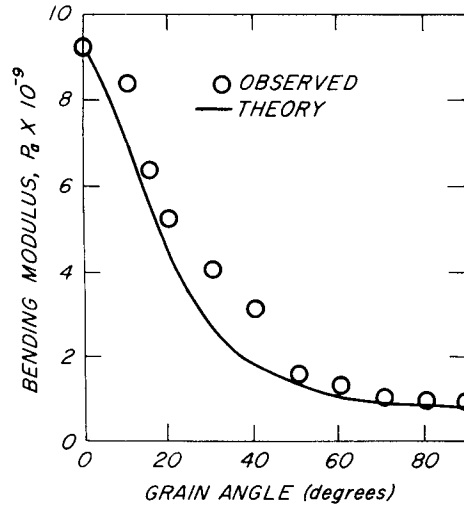


M 146 817

FIG. 7. Fracture energies obtained for specimens as a function of bondline thickness. G_{Ic} and G_{Ia} values are obtained from P_c and P_a values, respectively. Note the sharp rise near a bondline thickness of 100 microns and sharp decrease for bondline thicknesses less than 50–60 microns.

Samples made with the press design shown in Fig. 3B gave more uniform bondline thickness, and hence the values of P_c and P_a for these samples were much more constant. This design proved useful, especially for observing effects of grain angle of the wood beams reported later in this paper. Note that a good control of the bondline thickness could also have been achieved by gluing rectangular pieces of wood and subsequently machining them to the appropriate contour. We deliberately avoided doing this in order to eliminate fatigue cracking of joints.

In subsequent investigations the contour of the samples was changed to an m value of 0.52 cm^{-1} (1.33 inch^{-1}). For these samples the contour has a steeper slope that is nearly constant and can be approximated by a straight line taper. This design has several advantages: 1. it can be cut more easily with no special jigs; 2. the samples can be uniformly pressed during bonding even on the contoured section. The uniform pressure leads to uniform bondline thickness in the contour region (See Fig. 5C). Therefore, crack length measurements are not necessary, and this considerably reduces the effort in obtaining reproducible data. Figure 6C shows typical data obtained from such a sample geometry. Note the very uniform P_c and P_a value obtained on such samples in the contoured region. Also note that the values of P_c and P_a obtained on such samples are larger than those obtained with the original $m = 1.18 \text{ cm}^{-1}$ (3 inch^{-1}) specimens. However, the fracture energies calculated from the new m value and experimental P_c and

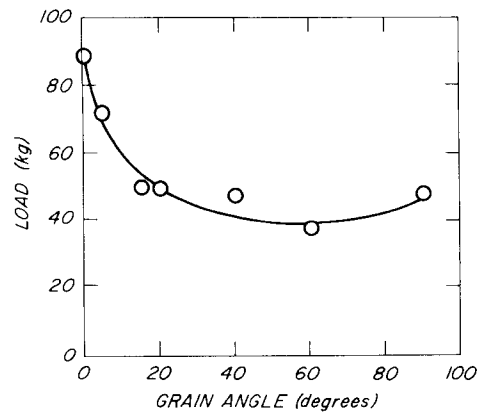


M 146 820

FIG. 8. The effect of grain orientation on the bending modulus of wood. The modulus was measured on beam samples cut from the contoured specimens used in the cleavage experiments.

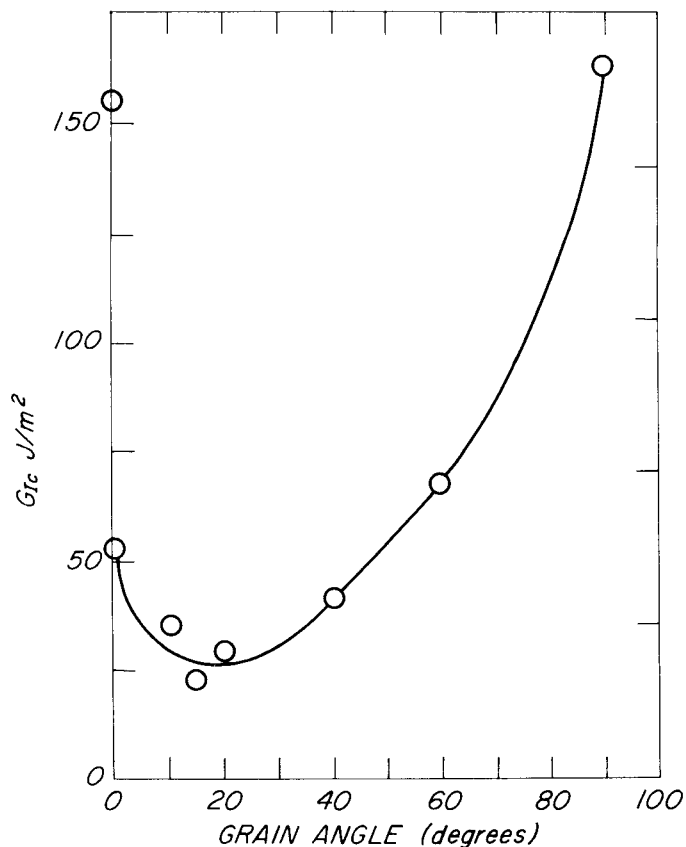
P_{ai} values correspond very closely with the values obtained from $m = 1.18 \text{ cm}^{-1}$ specimens. This indicates that G_{lc} and G_{la} are independent of beam contour.

After the samples were broken, visual examination of the samples fracture surfaces indicated major differences in the mode of failures. If the fracture energies were low (weak bond), the crack proceeded near the wood interface. Alternation of crack from one wood beam surface to another was observed. When high fracture energies were observed, either the crack proceeded down the middle of the bond or through the wood. This was especially evident for the wood-bonding studies involving different grain angles.



M 146 819

FIG. 9. Effect of grain orientation (with respect to bondline) on crack initiation load, P_c .



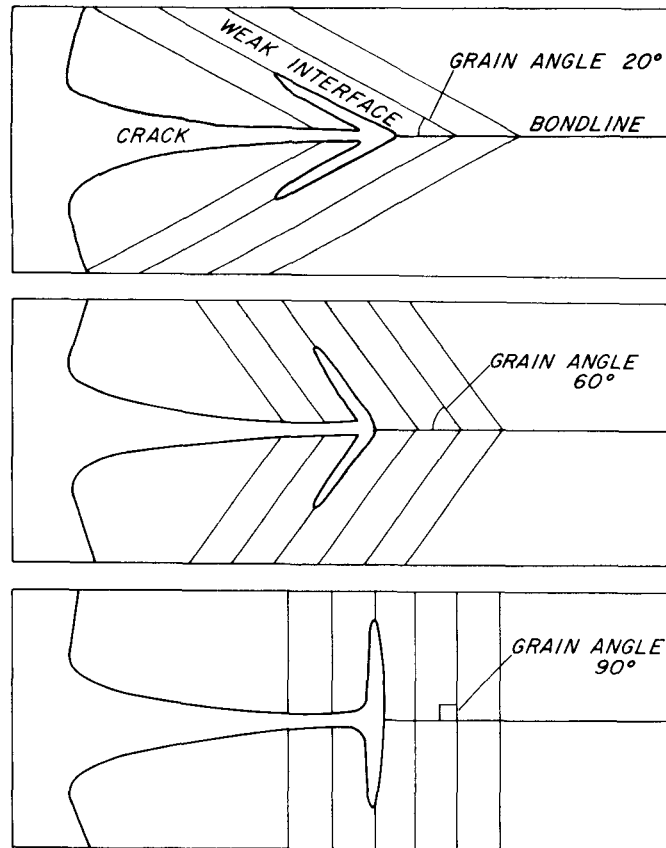
M 146 807

FIG. 10. Variation of fracture energy with grain angle. Inclusion of the bending modulus of beams as a function of grain angle gives high values of fracture energy as the grain angle is increased to 90 degrees. Predominance of cohesive, middle of bond, failure was observed for specimens having grain angles of 90 degrees.

Effect of grain angle

Specimens were prepared so that the wood grain of the two adherends converged at an angle to the plane of the glueline. Specimens with grain angles of 0° , 5° , 10° , 15° , 20° , 40° , 60° , and 90° were used in this study. On completion of experiments, uniform beams of dimensions of $1.27 \times 3.35 \times 15.08$ cm were used to determine the variation of bending modulus with grain angle. Figure 8 gives a comparison of the results of these experiments with theoretical prediction using Hankinson's formula.

Figure 9 shows a plot of variation of crack initiation loads with grain angle. It can be seen that crack initiation loads were highest for the zero degree grain angle and decreased to a somewhat constant value as the grain angle increased to 90 degrees. However, insertion of the appropriate values of load and modulus into Eq. 4 gave interesting values for G_{1c} . Figure 10 shows that G_{1c} decreases as the

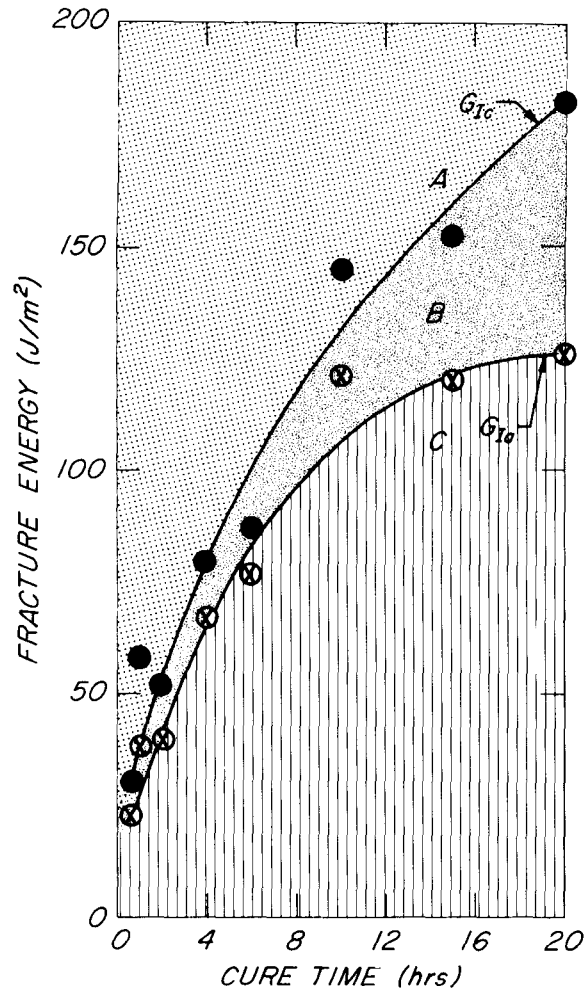


M 148 126

FIG. 11. Effect of opening of weak interface along the grain at increasing angles to the bondline and the direction of the principal crack direction. Cracktip at failed interface becomes more blunt as grain angle increases.

grain angle is increased from zero degrees, goes through a minimum at about 20 degrees grain angle, and increases thereafter. This behavior is similar to that observed by Ruedy (1977). Visual observation of the surfaces of adherends after cleavage revealed that the crack migrated between the surfaces of adherends as grain angle is increased from zero degrees. At 90° grain angle, a true center-of-bond failure occurred.

The variation of G_{1c} with grain angle may be attributed to a combination of three factors: the total area available for contact between the adhesive and wood, the extent of adhesive penetration into the adherends, and the ease of fiber-fiber (wood) separation and/or ease of adhesive-wood interface delamination. Assuming that the cell lumens are not blocked during surface preparation prior to bonding, the depth of adhesive penetration and the area of contact between the adhesive and wood will increase as the grain angle is increased from zero to 90 degrees. Cook and Goodon (1976) have described a weak interface mechanism



M 146 810

FIG. 12. Change of G_{1c} and G_{1a} due to cure time at a 70 C oven temperature. Note increase of G_{1c} - G_{1a} with cure time indicating greater brittle behavior. Grain angle = 20°.

for crack-stopping. According to this mechanism, an interface that is at approximately 90 degrees to the plane of the crack and whose strength is less than one-fifth of the general cohesive strength of the material, will be broken before the main crack reaches it. Such delamination effectively stops and blunts the crack. Reinitiation of the blunted crack requires expenditure of a large amount of energy. Consequently, such delamination results in an increase of fracture strength. Wood is generally at least ten times stronger in tension along the grain than across it. At 90 and zero degree grain angles, the grain orientation may be such that the tensile stresses induced perpendicular to the crack plane can cause wood-wood separation and/or adhesive-wood interface delamination. Consequently, the fracture energies at these grain orientations are high (Fig. 11). At intermediate

grain angles, the extent of delamination (and hence fracture energies) is much lower. We are currently trying to determine the exact magnitudes of the stresses required to induce these delaminations by computer simulation utilizing the stress transformation equations for orthotropic materials.

Two important conclusions can be drawn from these results:

1. Using crack initiation, loads or stresses calculated from them for design purposes can lead to erroneous results. G_{1c} is a better design parameter because this takes into account the orthotropic nature of wood.
2. It appears that adherends with grains oriented at 90° to the plane of the glue line will give the cohesive strength of an adhesive.

Effect of cure time

Figure 12 shows a strong effect of cure time on fracture energy. Furthermore, the difference between crack initiation and crack arrest values for the system increases as cure time increases. This behavior has also been observed in previous investigations for wood-epoxy systems as reported by Mijovic and Koutsky (1979). The difference between G_{1c} and G_{1a} can be related to the brittleness of the cured system. The raw load-deflection data indicate greater crack instability at long cure times.

The usefulness of this test method for design purposes can be seen from Fig. 12. The G_{1c} and G_{1a} data curves divide the fracture energy-cure time relationship into three regions A, B, C as shown. For loads applied to specimens producing G_1 values in region A, i.e., greater than G_{1c} , catastrophic failure will occur. Loads applied to specimens producing G_1 values in region B are capable of crack arrest and therefore failure will be erratic and highly dependent on the environment. Loads applied to specimens producing G_1 values in region C result in no crack growth.

We have performed initial dead-load tests on specimens of $m = 1.18 \text{ cm}^{-1}$ (3 inch⁻¹) at 25 C and varying humidities. Sharp, reproducible pre-cracks were achieved by preloading the specimens, and the corresponding G_{1c} values were determined. The specimens were then dead-loaded to induce G_1 levels 50 to 95% of the G_{1c} measured in the preload. At low applied dead loads (i.e. equivalent to 50% of G_{1c}), crack growth was not observed with change of environment, especially humidity, representing behavior in region C. However at high applied loads (i.e. equivalent to 95% of G_{1c}), intermittent crack growth—and in some cases failure—was observed with fluctuations in environmental conditions.

This type of testing could be important in prediction of durability. Changes in fracture properties with increasing cure times at elevated cure temperatures may be indicative of changes in fracture properties of specimens at lower service temperatures over longer periods of time. An important unanswered question is the effect of temperature and time on G_{1c} and G_{1a} and their differences.

REFERENCES

- BASCOM, W. D., R. D. COTTINGTON, AND R. L. JONES, 1975. The fracture of epoxy and elastomer-modified epoxy polymers in bulk and as adhesives. *J. Appl. Polym. Sci.* 19:2542-2562.
- BENNETT, S. J., K. L. DEVRIES, AND M. L. WILLIAMS, 1974. Adhesive fracture mechanics. *Int. J. Fracture* 10:33-43.

- COTTRELL, A. M. 1959. Theoretical aspects of fracture. Technology Press, New York.
- GLEDHILL, R. A., AND A. J. KINLOCH, 1974. Environmental failure of structural adhesive joints. *J. Adhesion* 6:315-330.
- GOTDON, J. E. 1976. The new science of strong materials. Penguin, New York, pp. 112-120.
- GRIFFITH, A. A. 1920. The phenomena of rupture and flow in solids. *Trans. Roy. Soc. London* A221:163-198.
- IRWIN, G. R. 1958. Fracture—Encyclopedia of physics, v. 6. Springer-Verlag, Berlin. Pp. 551-562.
- JOHNSON, J. A. 1973. Crack initiation in wood plates. *Wood Sci.* 6(2):151-158.
- MUOVIC, J. S., AND J. A. KOUTSKY, 1979. Effect of wood grain angle on fracture properties and fracture morphology of wood-epoxy joints. *Wood Sci.* 11(3):164-168.
- MOSTOVOY, S. AND E. J. RIPLING, 1975. Flaw tolerance of a number of commercial and experimental resins. *Adhesion Sci. Technol.* 93:513-562 (edited by P. H. LEE, Plenum).
- RIPLING, E. J., S. MOSTOVOY, AND R. L. PATRICK. 1964. Measuring fracture toughness of adhesive joints. *Mater. Res. Stand.* 4:129-134.
- RIVER, B. H. 1978. Measurement of shear modulus and shear strength of adhesives. Forest Products Laboratory Communication, Madison, Wisconsin.
- RUEDY, T. C. 1977. The effect of grain angle orientation on the fracture toughness of wood adhesive systems. M.S. Thesis, Forestry and Forest Products, Virginia Polytechnic Institute and State University.
- STRICKLER, M. D., AND R. F. PELLERIN, 1973. Rate of loading effect on tensile strength of wood parallel to the grain. *For. Prod. J.* 23(10):34-36.
- WILLIAMS, M. L. 1969. The continuum interpretation for fracture and adhesion. *J. Appl. Polym. Sci.* 13(1):29-40.